ACS APPLIED MATERIALS & INTERFACES

Research Article

www.acsami.org

An Integrated Microsystem for Real-Time Detection and Threshold-Activated Treatment of Bacterial Biofilms

Sowmya Subramanian,*[,†,‡] Ekaterina I. Tolstaya,[‡] Thomas E. Winkler,[†,§] William E. Bentley,[§] and Reza Ghodssi*[,†,‡,§]

[†]MEMS Sensors and Actuators Laboratory, Institute for Systems Research, [‡]Department of Electrical and Computer Engineering, and [§]The Fischell Department of Bioengineering, University of Maryland, College Park, Maryland 20742, United States

Supporting Information

ABSTRACT: Bacterial biofilms are the primary cause of infections in medical implants and catheters. Delayed detection of biofilm infections contributes to the widespread use of high doses of antibiotics, leading to the emergence of antibiotic-resistant bacterial strains. Accordingly, there is an urgent need for systems that can rapidly detect and treat biofilm infections in situ. As a step toward this goal, in this work we have developed for the first time a threshold-activated feedback-based impedance sensor-treatment system for combined real-time detection and treatment of biofilms. Specifically, we demonstrate the use of impedimetric sensing to accurately monitor the growth of *Escherichia coli* biofilms in microfluidic flow cells by measuring the fractional relative change (FRC) in absolute impedance. Furthermore, we demonstrate the use of growth measurements as a threshold-activated trigger mechanism to initiate successful treatment of biofilms using bioelectric effect (BE), applied through the same sensing electrode array. This was made possible through a custom program that (a) monitored the growth and removal of biofilms within the microfluidic channels in real-time and (b) enabled the threshold-based activation of BE treatment. Such BE treatment resulted in a ∼74.8 % reduction in average biofilm surface coverage as compared to the untreated negative control. We believe that this smart microsystem for integrated biofilm sensing and treatment will enable future development of autonomous biosensors optimized for accurate real-time detection of the onset of biofilms and their in situ treatment, directly on the surfaces of medical implants.

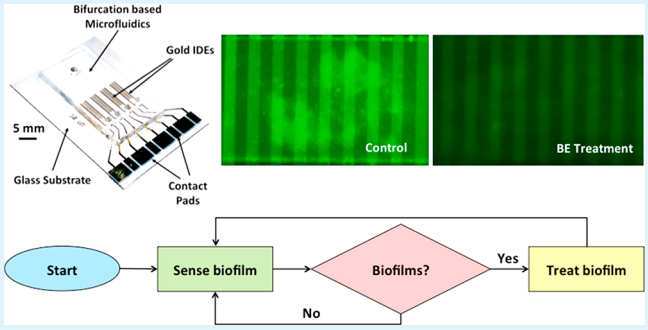

KEYWORDS: *bacterial biofilms, interdigitated microelectrodes, impedance sensing, bioelectric effect, microfluidics, microsystem*

1. INTRODUCTION

Currently, it is estimated that approximately 50−60% of the total hospital acquired biofilm infections detected annually in the United States are related to indwelling medical devices.[1] There is often a long period between the onset of biofilm formation and the symptomatic detection of the infection,[2] leading to medical complications and expensive invasive revisional surgeries, increasing the financial burden on the patient. Additionally, the treatment of biofilm infections using antibiotics prior to the formation of a thick extra cellular matrix (ECM) (i.e., right at the onset of infection) would ensure the need for only small doses of antibiotics for a shorter duration of time. Hence, accurate and sensitive sensors for timely detection of biofilm formation are highly desirable.

Bacterial biofilms are one of the most common causes of persistent infections in medical implants and catheters.[3,4] These infections are formed when freely floating bacteria adhere onto a surface and, through a chemical communication process known as quorum sensing (QS), envelop themselves in a slimy layer termed the extra cellular matrix (ECM).[5−7] The ECM prevents the diffusion of antibiotics into the biofilm through various active and passive cellular mechanisms, thereby adding to any existing antibiotic resistance of the bacteria and resulting in much higher antibiotic resistance than planktonic bacteria.[8−12] The resulting higher antibiotic resistance of biofilms has led to the use of very high doses of antibiotics as treatment (500× to 5000× the minimum inhibitory concentration (MIC)) in nonclinical studies.[13−15] Such high antibiotic concentrations are practically impossible to achieve in clinical settings using conventional antibiotic therapies due to associated toxicities and side effects and the limitation of renal and hepatic functions. Nevertheless, the widespread use of significantly higher than MIC levels of antibiotics has also contributed to the emergence of antibiotic resistant bacterial strains,[9] thus compelling research into alternative methods of treatment that are not based solely on high doses of antibiotics.

Research in the field of biosensors has made available a variety of technologies for the detection of minute amounts of biological samples, including biofilms.[16−28] Optical methods for studying biofilms have been used for macroscopic and

Received: April 5, 2017
Accepted: August 17, 2017
Published: August 17, 2017

DOI: 10.1021/acsami.7b04828
ACS Appl. Mater. Interfaces 2017, 9, 31362−31371

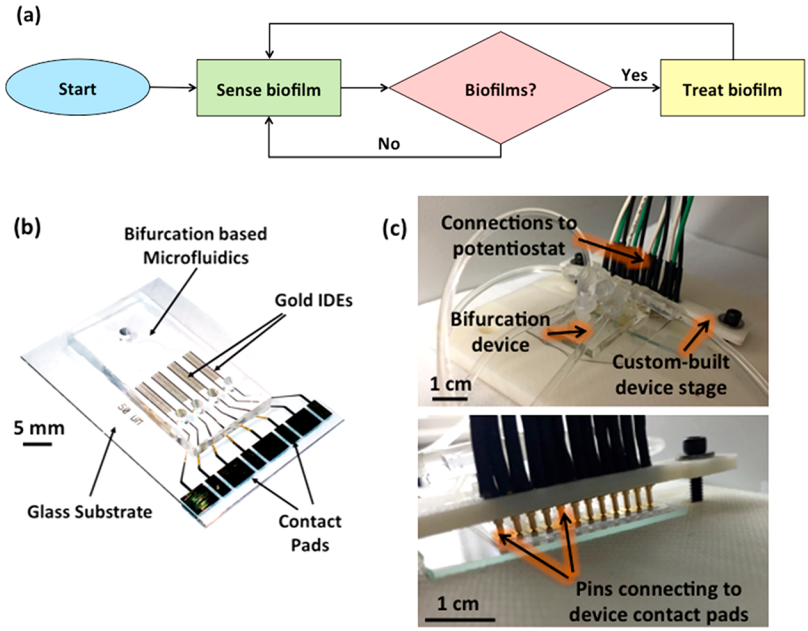

Figure 1. (a) Flowchart of proposed feedback to actively switch from sensing to treatment mode. (b) Photograph of microfluidic bifurcation device integrated with IDE sensors (scale bar = 5 mm). (c) Custom stage for interfacing up to two bifurcation devices to the potentiostat (scale bars = 1 cm).

microscopic studies.[29,30] However, a major disadvantage of optical sensors is the difficult integration and packaging of the biosensor components into a small footprint for simple use with medical implants. A method to address the concerns associated with three-dimensional optical systems is using a surface acoustic wave (SAW) sensor that enables sensitive real-time detection of biofilm formation.[31,32] The change in resonant frequency of the sensor gives a direct measure of bacterial loading on the surface. Nevertheless, this system required the use of piezoelectric material that is usually not biocompatible, thus requiring the use of effective passivation layers and increasing the complexity of the device.

Impedance based techniques have been used as a method of transduction for detecting and/or quantifying bacteria. Specifically, impedance microbiology (IM) has been used for decades to detect the presence of microorganisms in samples in the food industry, environment, health care, etc.[33,34] IM is based on the simple principle that the electrical parameters of the growth medium change with a change in microbial growth and metabolic activity. To detect bacterial growth in real time, the relative or absolute change in conductance, impedance, resistance, or capacitance of the electrolyte solution or the double layer capacitance at the electrolyte−electrode interface is measured at a given temperature using either macro- or microscale electrodes. This method has also been used for the detection of biofilm, as both cells and the ECM within the biofilm serve as a dielectric material, thereby providing an electrical impedance that varies with time or biofilm composition.[22,23,25]

Interdigitated microelectrodes (IDEs) have commonly been used for impedance based sensing of biological samples. IDE based systems have been shown to successfully detect pathogenic bacteria, antibodies, and other biological agents.[35,36] For example, Yang et al. demonstrated the use of IDEs for sensing bacterial growth by detecting a 30% change in the double layer capacitance and almost no change (−0.58%) in the medium capacitance.[35] The advantages of using IDE based impedance systems include a reduction in sample volume, low resistance, high signal-to-noise ratio, and the rapid attainment of steady state.[34]

Research into new treatments for biofilm has branched into the fields of material sciences, electrical engineering, and bioengineering. Some examples of biofilm treatment methods include antibiotic and antimicrobial release from material surfaces,[37−39] surface modifications to prevent bacterial adhesion,[40−43] small molecule inhibitors to actively prevent ECM formation,[44−46] and the bioelectric effect (BE) or the combination of electric fields with low dosage antibiotics. While all these treatments show promise, the BE treatment is inherently interesting as it can be easily integrated with electronic sensor systems. BE studies reveal that low strength electric fields when combined with near MIC levels of antibiotics result in a synergistic removal of biomass.[47−51] While the exact mechanism of action is not understood, many hypotheses including increased antibiotic penetration into the ECM, change in local pH, generation of radicals, etc. have been suggested.

Presented here is a novel integrated IDE microsystem that enables label-free and real-time detection of bacterial biofilm growth as well as threshold-activated biofilm treatment using BE. Our previous work with BE applied a 500 mV electrical signal during the entire treatment period,[52,53] a long-term biocompatibility concern for medical devices that on average require treatment over days. Additionally, the use of mechanical (or optical) and electrical domains for monitoring and treatment respectively made essential the use of auxiliary electrodes for BE application, increasing device footprint and necessitating additional bulky equipment.[52,53] Here, we demonstrate that biofilms can be accurately sensed in real time by measuring the change in impedance across the IDEs. Treatment is performed, for the first time, by applying a 100 mV signal across the same IDEs in combination with near MIC levels of antibiotic (BE). This BE is applied to each channel at regular intervals for only $\sim^1/_7$ of the total 24 h treatment

DOI: 10.1021/acsami.7b04828
ACS Appl. Mater. Interfaces 2017, 9, 31362−31371

period, a significant decrease in biofilm treatment time. Additionally, we also show the real-time monitoring of threshold-activated biofilm BE treatment. This was achieved using a custom algorithm that enables the IDEs to sense the growth of biofilms, which is in turn used as a trigger to initiate BE treatment, which is applied using the same IDEs. This closed-loop feedback system referred to as "feedback-based real-time threshold-activated biofilm treatment'" allowed setting of various crucial treatment parameters so that BE is applied only for a small fraction of the total treatment period. This closed-loop feedback is presented in the flowchart of Figure 1a. Contrary to former systems, this integration of sensing and BE treatment capabilities into purely the electrical domain provides an elegant microsystem solution toward rapid, autonomous treatment of biofilms.

Furthermore, we evaluate the efficacy of this combinational treatment using *Escherichia coli* biofilms as the model organism and compare the results of the treatment with control, antibiotic-only, and electric field-only therapies when applied to uniform biofilms. However, the same combination treatment is also effective in treating biofilms consisting of other types of bacteria, as the specificity of the treatment depends on the antibiotic(s) used.[48,54−56]

While impedance sensors, including IDE sensors, for the detection of biofilm growth have been proposed in the past,[57−59] they have been used to detect growth in static environments like microliter plates or Petri dishes or in macroscopic setups like the CDC reactor. However, we demonstrate herein the detection of biofilm growth in microfluidic cells that operate in dynamic flow conditions. To ensure that similar experimental growth conditions were applied to all microfluidic channels at any given point in time, multiple experiments were performed in parallel using bifurcation-based microfluidics.[60] End-point fluorescence microscopy results correlate with the fractional relative change (FRC) in impedance measured using our system. This sensor-treatment microsystem, we believe, will facilitate development of automated sensors that are optimally designed not only for the rapid and sensitive detection of the onset of biofilm infections but also for in situ treatment.

2. MATERIALS AND METHODS

Device Fabrication and Design. The impedance sensor was fabricated by evaporating Cr/Au (20 nm/180 nm) on a Pyrex wafer followed by a wet etch process to form the IDE pattern. IDEs with two different widths, 50 and 100 μm, with the electrode width equal to the spacing, were fabricated. Following this, the devices were diced and immersed in piranha solution (3:1 of H_2SO_4/H_2O_2) for 1 min and then rinsed with deionized (DI) water and blow-dried using nitrogen. Microfluidic channels were fabricated using traditional soft lithography techniques[61] and were cast from polydimethylsiloxane (PDMS) (1:10 ratio of curing agent to polymer) molded by photopatterned KMPR-1050. The microfluidic channels are 100 μm deep, 500 μm wide, and 2 cm long. Holes were punched at the inlet and outlet of each channel using a 2 mm dermatological punch. The channels were then aligned over the impedance sensor and irreversibly plasma-bonded to the device as shown in Figure 1b. To enable fluid flow, the microfluidic channel was interfaced to the external fluidic components using flexible Tygon tubing and barbed connectors. The tubing at one end of the device was connected to a syringe pump (Cole Parmer 74901) operating in infusion mode at 20 μL/h; at the outlet the tubing was inserted into a microcentrifuge tube for waste collection. Each device was then sterilized by flowing 70% ethanol for 1 min and rinsed with DI water. The entire apparatus was kept in an incubator held at 37 °C.

Device Preconditioning and Growth Media Baseline. Device preconditioning was accomplished by flowing 1× phosphate buffered saline (PBS) through the channel at 20 μL/h for 24 h. Any air bubbles trapped in the channels were flushed to the outlet by increasing the flow rate to 100 μL/min for a short period of time. The primary goal of preconditioning was to allow for acclimatization of the device to the change in environment from air to liquid so as to achieve a stable impedance signal. It also enabled removal of any excess ethanol or trapped air bubbles present in the channel, tubing, and connectors. Following this, fresh growth medium (Lysogeny broth (LB)) was introduced into the channel at 100 μL/min until the entire channel was filled with LB. Impedance measurements were obtained in real time during both the preconditioning and LB medium baseline periods. The details of the impedance measurement setup are discussed in the "Experimental Setup" subsection of this section.

Biofilm Growth. A bacterial suspension of *Escherichia coli* K-12 W3110[62] was prepared from a stock solution stored at −80 °C. The suspension was prepared by transferring a frozen sample of bacteria into 5 mL of LB medium in a cell culture tube. The tube was then placed in an incubator-shaker (New Brunswick Innova 4000) at 250 rpm and 37 °C for 18−20 h to allow for bacterial growth. Subsequently, sterile LB medium was used to dilute the suspension to a final OD_{600} of ∼0.25. The diluted suspension was sealed in a biosafety cabinet and was then injected into the sterilized microfluidic channels at a rate of 100 μL/min. The suspension was allowed to seed the channel for 2 h without flow to facilitate bacterial attachment to the glass substrate. Fresh growth medium (LB) was then supplied continuously to the channels for 24 h at a rate of 20 μL/h. This flow rate was chosen as it was characterized and confirmed during our previous work to be sufficient to supply adequate nutrients for biofilm growth.[63] This protocol resulted in the formation of uncontaminated mature *E. coli* biofilms.[31,52,53,63] Impedance measurements were obtained periodically in real time during the seeding and growth phases every 10−15 min.

Biofilm Treatment. After the 24 h growth, antibiotic treatment (for the antibiotic only and BE treatment channels) or pure LB medium (for the negative control and E-field only channels) prepared and sealed in a sterile environment was applied to the biofilms for an additional 24 h. While clinical biofilm growth may occur over longer time periods like weeks or sometimes even months, for the purposes of the present study we chose biofilm growth and treatment periods of only 24 h each in order to reliably compare the antibiotic-free treatment results with other previously published treatment results.[53] The antibiotic gentamicin, which is commonly used for treating *E. coli* infections, was diluted in LB to a final concentration of 10 μg/mL (2 × MIC). This diluted solution of the antibiotic or fresh LB was introduced into the channels at a flow rate of 20 μL/h. Real-time impedance measurements were obtained while applying both treatments to the biofilms. After 24 h, the biofilms were stained using the Filmtracer LIVE/DEAD biofilm viability kit (Life Technologies Inc.), using equal proportions of SYTO9 and propidium iodide diluted in DI water, introduced at 20 μL/h. The biofilms were then washed with DI water at the same flow rate to remove any excess stains and imaged using a fluorescent microscope (Olympus BX60). The obtained images were analyzed using an image processing software (ImageJ 1.44), enabling assessment of the background subtracted image and an impedance-independent quantitative measurement of the biofilm surface coverage.

Experimental Setup. Multiple experiments were performed in parallel using bifurcation-based microfluidics to ensure similar experimental conditions were applied to all channels at any given point in time.[60] A custom stage, shown in Figure 1b, was machined to interface the bifurcation device to the measurement system. A potentiostat (model 660D, CH Instruments Inc.), with multiplexing capabilities (CHI684 multiplexer, CH Instruments Inc.) was used to serially measure the ac impedance of each of the interfaced IDE sensors every 10−15 min. However, instead of directly gathering impedance data using the CH Instruments (CHI) software, the potentiostat and multiplexer were controlled by a custom-built software, developed using MATLAB, that enabled both real-time

DOI: 10.1021/acsami.7b04828
ACS Appl. Mater. Interfaces 2017, 9, 31362−31371

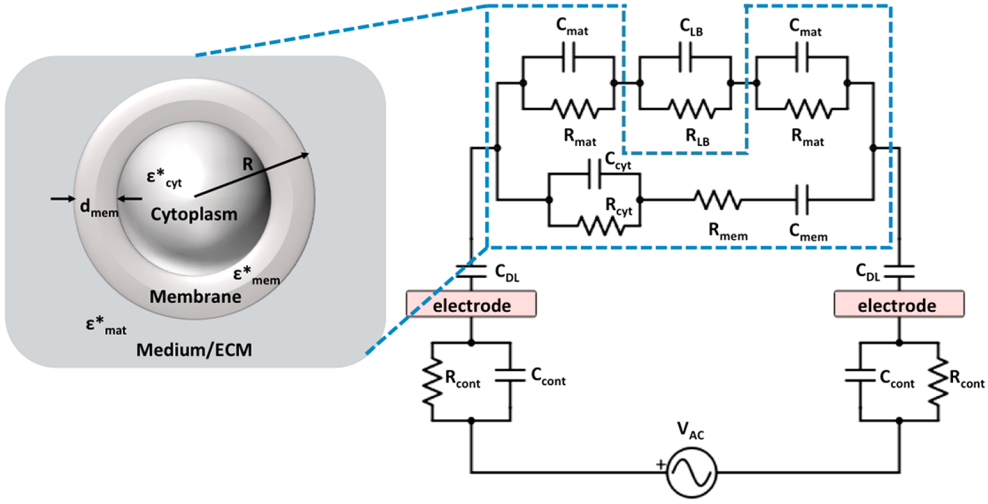

	Conductivity (S/m)	Relative Permittivity	Reference
Cell cytoplasm	0.19	61	67,68
Cell membrane	5×10^{-8}	10.8	67,68
ECM	0.68	60	69
LB media	0.754	78	70

Figure 2. Effective medium approximation of a bacterial cell as a single-shelled sphere (top left), the equivalent circuit of the experimental setup (top right), and table of parameters used in the simulation (bottom). The part of the equivalent circuit boxed in blue corresponds to the MMT based approximation of the biofilm, where R_{cont} and C_{cont} are the electrode contact resistance and capacitance, C_{DL} is the double layer capacitance, R_{cyt} and C_{cyt} are the cytoplasmic resistance and capacitance, R_{mem} and C_{mem} are the resistance and capacitance of the membrane, R_{mat} and C_{mat} are the extracellular matrix (ECM) resistance and capacitance, and R_{LB} and C_{LB} are the growth medium (LB) resistance and capacitance.

impedance monitoring and the application of electric field (E-field) based treatments in any of the channels of the device based on user-defined inputs. Impedance measurements were obtained by applying an ac signal of 5 mV at the user-provided sensing frequency of 100 Hz across the IDEs and measuring the generated current. This frequency was chosen based on previous experimental optimizations for signal-to-noise ratio. Due to hardware restrictions of the potentiostat's multiplexer, a maximum of four sensors could only be tested in parallel. Photographs of the device and the setup are shown in Figure 1b,c. All microfluidic devices were placed in an incubator, and experiments were performed at 37 °C.

Data Acquisition and Feedback Control Macro. A graphical user interface (GUI) was developed using MATLAB for the user to provide the required inputs to perform the experiment. The GUI was implemented using the libec SDK for MATLAB, provided by CH Instruments. Although other platform libraries like LabVIEW are available, MATLAB was chosen because of the relative ease in programming, high functionality, and its ubiquitous use in research.

Supporting Information Figure S1a presents a screenshot of the MATLAB module GUI that appears upon running the MATLAB file. Upon execution of the macro, the library SDK is compiled using the inputs provided through the GUI to control the potentiostat. Two additional windows, shown in Figure S1b, are also displayed alongside the GUI. These two windows contain eight graphs in total and plot the absolute impedance and the FRC in impedance in real time, respectively, for each channel listed in the List Channels field. The GUI allows the user to collect and visualize the impedance data gathered in four experimental modes, viz., Conditioning, Control, Seeding, Growth, Sensing, and BE Treatment. It is important to note that the threshold-activated treatment is applied only during the BE Treatment experimental mode. Table S1 of the Supporting Information lists all the inputs that are to be provided by the user into the MATLAB GUI along with a brief description of each field and their default values. A comprehensive explanation of each input to the GUI and the details of each mode of operation to successfully demonstrate threshold-activated treatment can be found in the Supporting Information. Furthermore, the verification of the functionality of the MATLAB module was performed through a simulated biofilm growth experiment. The details of the experimental verification and its results (Figure S2) are presented in the Supporting Information.

Finite Element Modeling. To model the impedance system, a 3D electrodynamic simulation was set up in COMSOL Multiphysics (version 5.0, COMSOL Inc.). The simulation covered a microfluidic channel segment of length 400 μm, width 50 μm, and height 100 μm. The simulation results were scaled up to the final channel width of 500 μm by multiplying by the appropriate scaling factor. Within the channel is a pair of gold electrodes whose width and spacing can be varied. Three sets of electrodes with equal widths and spacings, viz. 25 μm, 50 μm, and 100 μm, were simulated. For simplicity it was assumed that a biofilm of uniform thickness (5−30 μm) containing 10% bacterial cells and 90% ECM, grows along the entire length of the channel. The remaining channel volume was modeled to simulate LB growth medium. Although the electrical characteristics of the LB medium change with bacterial metabolism, for the case of this simulation it was assumed that the channel was filled with fresh LB at all times. This represents the experimental condition in which the microfluidic flow rate is high enough to ensure that the medium in the

DOI: 10.1021/acsami.7b04828
ACS Appl. Mater. Interfaces 2017, 9, 31362−31371

channel is replaced often and always guaranteed to be a nutrient-rich environment. The contact capacitance (C_{cont}) and resistance (R_{cont}) and the double layer capacitance (C_{DL}) formed at the electrodes were also included as part of the simulation.

The dielectric properties of the biofilm depend on the electrical parameters (the permittivity ε and the conductivity σ of the biofilm's individual components and their volume fractions).[64−66] The complex dielectric constant of the biofilm was calculated using eq 1, derived from the well-established Maxwell's mixture theory (MMT), by assuming the biofilm to be a collection of spherically shaped objects (the bacterial cell), covered by a single shell (the cell membrane) and uniformly distributed in a medium (the ECM) as shown in Figure 2.[65]

$$\varepsilon^*_{biofilm}(\omega) = \varepsilon^*_{mat}(\omega)\frac{2(1-\varphi)\varepsilon^*_{med}(\omega) + (1+2\varphi)\varepsilon^*_{eq}(\omega)}{(2+\varphi)\varepsilon^*_{med}(\omega) + (1-\varphi)\varepsilon^*_{eq}(\omega)} \quad (1)$$

Herein, $\varepsilon^*_{eq}(\omega)$ is the equivalent complex dielectric constant of the dispersed particles (here bacterial cells) and can be written as

$$\varepsilon^*_{eq}(\omega) = \varepsilon^*_{mem}(\omega)\frac{2(1-\vartheta)\varepsilon^*_{mem}(\omega) + (1+2\vartheta)\varepsilon^*_{cyt}(\omega)}{(2+\vartheta)\varepsilon^*_{mem}(\omega) + (1-\vartheta)\varepsilon^*_{cyt}(\omega)} \quad (2)$$

For both equations, $\varepsilon^*_{mat}(\omega) = \varepsilon_{mat} + \sigma_{mat}/(i\varepsilon_v\omega)$ is the complex permittivity of the ECM, $\varepsilon^*_{mem}(\omega) = \varepsilon_{mem} + \sigma_{mem}/(i\varepsilon_v\omega)$ is the complex permittivity of the bacterial cell membrane, and $\varepsilon^*_{cyt}(\omega) = \varepsilon_{cyt} + \sigma_{cyt}/(i\varepsilon_v\omega)$ is the complex permittivity of the cellular cytoplasm. ε_v is the dielectric constant of free space, ω is the angular frequency of the applied potential, φ is the fractional volume of the bacterial cells. Although more accurate models like the ellipsoidal or cylindrical models are available, for the first order simulation presented here the bacterial cell was modeled as a sphere and assumed to have a radius R and a cell membrane of thickness d_{mem}. The parameter ϑ of eq 2 was calculated as $\vartheta = [R/(R + d_{mem})]$.[3] The complete equivalent circuit of the experimental setup, along with the values of the various parameters used to theoretically estimate the electrical properties of the biofilm, is shown in Figure 2. The portion of the equivalent circuit boxed in blue corresponds to the MMT based approximation of the biofilm, where R_{cont} and C_{cont} are the electrode contact resistance and capacitance, C_{DL} is the double layer capacitance, R_{cyt} and C_{cyt} are the cytoplasmic resistance and capacitance, R_{mem} and C_{mem} are the resistance and capacitance of the membrane, R_{mat} and C_{mat} are the extracellular matrix (ECM) resistance and capacitance, and R_{LB} and C_{LB} are the growth medium (LB) resistance and capacitance.

Substituting for $\varepsilon^*_{eq}(\omega)$ in eq 1 and separating the resultant complex equation into the real and imaginary parts, we arrived at the permittivity $\varepsilon_{biofilm}$ and the conductivity $\sigma_{biofilm}$ of the biofilm. The separation of the complex equation was performed using Mathematica (version 10.2.0.0, Wolfram Research). These equations were provided as input into COMSOL to obtain the impedance measured between the electrodes for a range of frequencies and spacings.

3. RESULTS

Simulation Results. The simulation results show that for IDEs with equal electrode width and spacing, the sensitivity of the sensors is inversely proportional to the width or spacing between the electrodes (Figure 3). This correlates with previous simulations that suggest that ∼90% of the electric field is contained within a height of one electrode width from the electrode surface.[71] Thus, for the same changes at the electrode surface, IDEs with smaller electrode widths show larger electric field change, and thus higher sensitivity, as compared to IDEs with larger electrode widths. Thus, 25 μm IDE sensors are more sensitive than 50 μm IDE sensors, which are in turn more sensitive than the 100 μm sensors. A similar trend in sensitivities was observed during our initial experiments. Since an increase in biofilm thickness occurs with growth time, the increasing simulated biofilm thickness along the x-axis of Figure 3 can be assumed to be an equivalent representation of increasing growth times. Thus, from Figure 3 we deduce that the time to saturation of the impedance signal is directly proportional to the electrode spacing. Therefore, 100 μm IDE sensors demonstrate the largest linear range over time but lowest sensitivity (slope of the initial line segment) when compared to 50 or 25 μm IDEs. In our experiments uniform biofilms are grown without the application of any treatment for 24 h to ensure reliable comparison of the different treatments applied to the microfluidic channels during the successive 24 h period. Consequently, a balance of both time to saturation and sensitivity of the device is required, and so the 50 μm IDE sensor was used for demonstration of impedance sensing and threshold-activated treatment of biofilms.

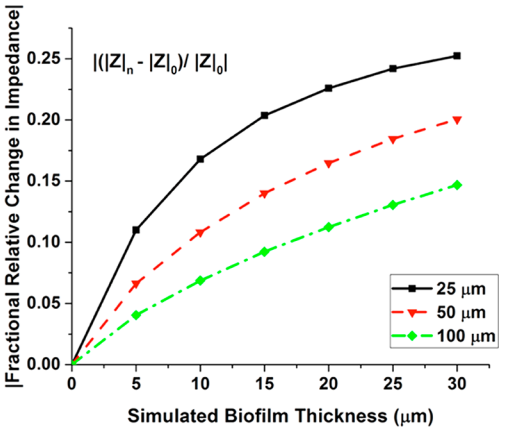

Figure 3. Magnitude of fractional relative change (FRC) in impedance at 100 Hz for the three different electrode widths and spacings with increasing biofilm thickness. The 25 μm IDE shows the highest sensitivity but the shortest time to signal saturation, whereas the 100 μm IDE results in the lowest sensitivity but the longest time to signal saturation.

PBS Conditioning. Figure S3 displays the fractional raw data output relative to $|Z|_{PBS\_Average}$ for the four channels of the bifurcation device at the end of the 24 h buffer conditioning. $|Z|_{PBS\_Average}$ of each channel was calculated by averaging all the nonoutlier data points collected during the entire PBS Conditioning mode for each channel. The FRC in magnitude of impedance at time t during the conditioning phase was then calculated as $(|Z|_t - |Z|_{PBS\_Average})/|Z|_{PBS\_Average}$. Any recorded data point if greater than a 100% change (fractional change greater than 1) with respect to the first data point was marked an outlier and removed from the plot. On average, there were one or two data points removed as outliers based on this criterion during the entire conditioning period. Additionally, in order to more clearly observe trends in the data, a moving average of the data was also calculated and plotted as a solid line, among the individual data points, in Figure S3 for each of the four channels. As perceived from the plots, the average FRC in impedance fluctuates during the first few hours (∼10 h) of the conditioning phase but stabilizes to near zero with time in all four device channels. Small fluctuations in measurements, as observed by the increase in impedance, were recorded over time and were verified to be a result of small visible air bubbles trapped within the microfluidic channels that were eventually removed with time or due to the intrinsic noise of the system. Also, different IDE sensors showed different levels of variation in signal initially, but eventually all signals stabilized close to

DOI: 10.1021/acsami.7b04828
ACS Appl. Mater. Interfaces 2017, 9, 31362−31371

zero. We hypothesize that this variation was due to difference in volume of the trapped visible air bubbles within the different channels of the bifurcation device.

Biofilm Growth. Figure S4 presents the fractional raw data output relative to $|Z|_{LB\ Baseline}$ at 100 Hz and the moving average (span of moving average = 5) from the Control phase through the end of the biofilm Growth phase of the experiment. The FRC in magnitude of impedance of each channel at time t during these experimental phases was calculated as $(|Z|_t - |Z|_{LB\ Baseline})/|Z|_{LB\ Baseline}$, where $|Z|_{LB\ Baseline}$ of each channel was calculated as the average of all the nonoutlier data points collected for the respective channel during the entire LB medium Control phase (solid black data points in Figure S4).

Following the PBS buffer conditioning, pure growth medium was introduced into the channels and the impedance data was measured for 6 h in the Control mode. Once at least 2 h of steady LB medium baseline signal (solid black data points in Figure S4) was established, an overnight culture of *E. coli* W3110 suspended in growth medium to a final OD_{600} of ~0.25 was introduced into the device to seed the microfluidic channels and allowed for bacterial attachment (no flow). The data obtained during the Seeding phase of the experiment was plotted in magenta in Figure S4. Subsequently, pure growth medium was introduced into the channels at 20 μL/h for 24 h to allow for uniform biofilm growth in all channels of the bifurcation device.[60] The real-time FRC in absolute 100 Hz impedance during biofilm Growth phase is plotted in green. These biofilms were highly uniform and enabled reliable comparison of the various treatments that were applied thereafter.

The plots presented in Figure S4 are the screen captures of the raw output data plotted on the MATLAB Figure 3 window screen at time point t = 26 h. Thus, there is no user-control over their axes limits due to the graphs each having different y-axis scales. Hence, the observed FRC in impedance between the four channels appears to vary significantly over time. This is primarily due to the large shifts observed in a few channels, viz. multiplexer channels 5 and 7, during the LB medium baseline or the bacterial seeding stages (0−8 h of the experiment), which we believe are due to the introduction of an air bubble in the channel. However, if these large initial shifts in impedance are removed, an equivalent net change in impedance is observed in all four channels from the start to the end of growth during which a continuous supply of growth medium is introduced into the microfluidic channels. Figure 4 plots this FRC in impedance for each of the four channels of the device during the growth phase, from approximately the 9 h to the 34 h time point, with respect to first data point measured in the Growth mode. The impedance decreases by about 0.10 during the first 10 h of the growth phase, which correlates with the initial rapid exponential increase in biomass of the biofilm during the first few hours of growth. Following the initial growth spurt, the rate of biofilm growth decreases, which is measured as a smaller decrease in impedance of 0.05 over the remaining 14 h. Eventually, equilibrium is attained between the biofilm growth and removal, due to shear stresses in the channel, which is recorded as an eventual leveling off of the impedance signal. This plot also highlights the near similar shift in impedance across all four channels of the device during the entire 24 h, which is suggestive of uniformity in biofilm growth across the channels. Additionally, it is worth noting that the near equal FRC in impedance observed in all channels of the device, presented in Figure 4, is similar to that obtained in other

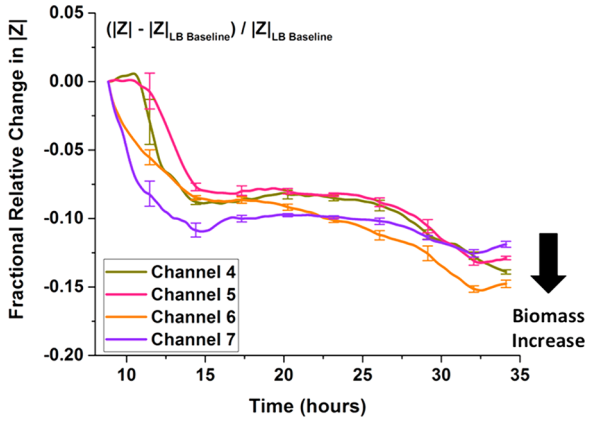

Figure 4. Measured real-time fractional relative change (FRC) in 100 Hz impedance across the four channels of the bifurcation device at the end of the growth phase. While the biofilm growth shows a decrease in impedance, the preceding baseline showed almost no change in measured impedance. The error bars plot the temporal change in biofilm at representative time points (span = 5).

repetitions of the experiment, thus highlighting the reproducibility of the impedance based sensing methodology to monitor biofilm growth in real time.

Threshold-Activated Biofilm Treatment. Following the growth of biofilms in all four channels of the device, different solutions, namely, LB or antibiotic (gentamicin 10 μg/mL in LB), were introduced into the microfluidic channels. The treatments applied to the channels of the device over 24 h are listed in the table in Figure 5. Channels 5 and 7 received the additional intervallic 100 mV ac electrical treatment in addition to the periodic 5 mV ac sensing voltage applied to all the channels. The decision to apply the 100 mV ac signal to both channels was made by the MATLAB macro using the impedance data gathered in the Sensing mode (blue data points). If the average Sensing mode data point was less than the user-defined threshold (blue data points are below the orange dashed line), the threshold-activated electric field treatment was applied, else the system continued in Sensing mode (macro functionality verification provided in Supporting Information Figure S2).

Figure S5 presents the FRC in absolute impedance at 100 Hz measured with a 5 mV ac signal for each of the four multiplexer channels for all experimental phases, i.e., Control (black), Seeding (magenta), Growth (green), and Sensing (blue), and BEtreatment (red).

Although BE treatment was provided at 100 mV ac, the final impedance measurement was performed at the end of each BE treatment cycle at 5 mV ac in order to accurately compare the results of the BE-treated with the other non-BE-treated channels. At the end of treatment phase, the untreated negative control channel (LB medium only of channel 4) and the E-field only treatment channel (channel 5) showed a further decrease in impedance, suggestive of an increase in total biomass or additional biofilm growth. Conversely, treatment with antibiotic (channel 6) and BE (channel 7) resulted in an increase in 100 Hz impedance, representing the removal or decrease in total biomass. It is worth noting that the threshold-activated treatment, represented by the red data points of channels 5 and 7, was periodically applied only during the treatment phase of the experiment, conditional to the measured FRC in

DOI: 10.1021/acsami.7b04828
ACS Appl. Mater. Interfaces 2017, 9, 31362−31371

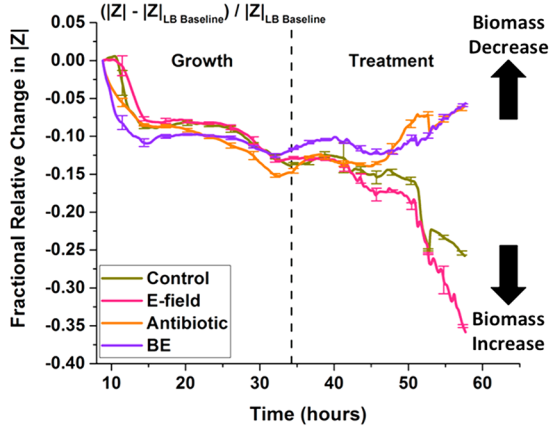

Channel No.	Treatment Name	Treatment Applied
4	Negative Control	LB media only
5	E-field Only	LB media + 100 mV at 1 MHz
6	Antibiotic	10 μg/mL gentamicin in LB media
7	Bioelectric Effect (BE)	10 μg/mL gentamicin in LB media + 100 mV at 1 MHz

Figure 5. Measured real-time fractional relative change (FRC) in 100 Hz impedance across the four channels of the bifurcation device at the end of the treatment phase. While the negative control channels (control and E-field only) show a decrease in impedance indicating further biofilm growth, biofilm treatments (BE and antibiotic) show an increase in impedance representing a decrease in total biomass. The error bars plot the temporal change in biofilm at representative time points (span = 5). The table lists the various experimental conditions applied to the microfluidic channels during the 24 h treatment period, over the 5 mV sensing voltage applied.

impedance being less than the user-defined Treatment threshold (orange dashed line in Figure S5).

For ease of comparing the channels, the processed FRC in 100 Hz impedance observed only during the growth and treatment phases is plotted in Figure 5. The data presented in this plot exclude any extreme outliers prior to performing a moving average (span = 5). This plot enables clear visualization and comparison of the change in 100 Hz impedance due to biofilm growth and treatment across all four channels of the device. As shown in Figure 5, the untreated negative control (olive line) and E-field only (pink line) treatments continue to measure a decrease in impedance, on average by a FRC in impedance of 0.20, even during the treatment phase, correlating with continued biofilm growth. In contrast, the antibiotic (orange line) and the BE (violet line) exhibit a change in the opposite direction, a measured FRC in absolute impedance of 0.10, indicating a decrease in biofilm biomass. It is also worth noting that the antibiotic treatment (orange line) appears to be as effective in treating the biofilm as the BE treatment, consistent with other two repeats performed. We hypothesize that the similar efficacies between the antibiotic and BE treatments is due to the periodic sensing voltage applied to the antibiotic treatment (channel 6) that also causes significant BE. Hence the efficacy of the treatment applied to channel 6 is not purely a result of only the antibiotic therapy but rather due to regular and recurring BE treatment that results in effective removal of the biofilm in the channel.

Optical Validation. To independently validate the results obtained using the impedance microsystem, end-point fluorescent images obtained for each channel of the device (for two identical repeats represented by the different patterned bar graphs) were analyzed using the image-processing program. Representative end-point optical micrographs of the negative control (LB medium only) and BE-treated (antibiotic and E-field) biofilms are presented in Figure 6a,b. ImageJ analysis shows that the antibiotic and the BE treatment reduced the average biofilm surface coverage across the two experimental repeats on average by ∼67.3% and ∼74.8%, respectively, compared to the untreated negative control (Figure 6c).

Thus, these results combined demonstrate that the microsystem can accurately measure the real-time change in impedance during the growth and removal of biofilms. Moreover, we have demonstrated that using a MATLAB module, the sensor's IDEs can be used to perceptively apply the electrical signal necessary to initiate BE treatment. Such effective treatment, using low amplitude signals and smaller treatment times, highlights the efficiency of this microsystem to sense and treat in situ bacterial biofilms concurrently.

Thicker biofilms are also prevented and treated. The developed microsystem switches to application of high E-field BE (100 mV E-field) when the most recent impedance measurement is more negative than the user-defined threshold.

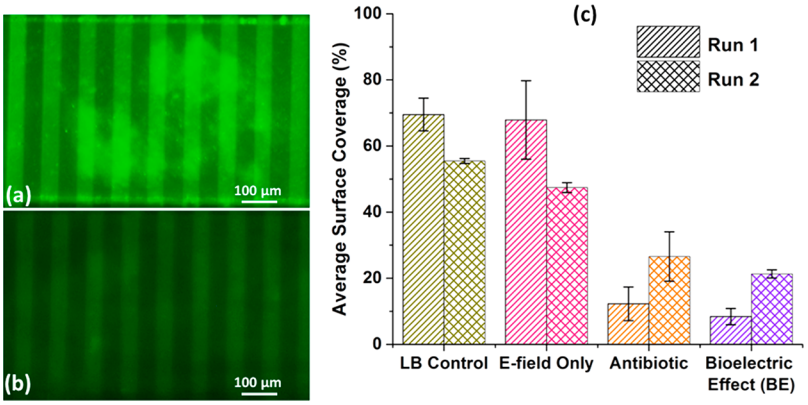

Figure 6. Representative micrographs of (a) untreated negative control and (b) BE treated biofilm imaged after the 24 h threshold-activated treatment cycle (scale bars = 100 μm). (c) Percentage average surface coverage as measured using ImageJ (N = 3 images/repeat) for two repeats (striped and checkered bars correspond to the two independent data sets). The background fluorescence exhibited by the gold IDE electrodes was subtracted during surface coverage analysis.

DOI: 10.1021/acsami.7b04828
ACS Appl. Mater. Interfaces 2017, 9, 31362−31371

This is continued until the measured impedance becomes higher than the set threshold value. This method of treatment with BE at the onset of biofilm formation ensures that thick biofilms are not formed. Our results also suggest that even the small periodic 5 mV ac signal used for probing the impedance between the IDEs results in enhanced treatment based on the principles of BE, leading to a dual approach for BE treatment application. While the first occurs concurrently during sensing, the second approach is through the biofilm growth-triggered threshold-activated BE treatment, applied using the custom-built macro. The latter could be used to help treat significantly thicker and more mature biofilms, which require a much stronger electrical signal energy for effective BE treatment.[72] This is a substantial advantage over our previous work with BE that applied a 500 mV electrical signal during the entire treatment period causing a long-term biocompatibility concern for medical devices, as they often require treatment over several weeks.[52] Thus, in contrast to former systems, this integration of sensing and BE treatment capabilities into an exclusively electrical domain provides an elegant microsystem solution for accurate threshold-activated sensing and treatment of biofilms.

4. CONCLUSION

We have presented a novel integration of sensing and treatment modules into an impedance-based microsystem. The developed platform is the first impedimetric microsystem for real-time monitoring and threshold-activated treatment of bacterial biofilms in a microfluidic bifurcation device. It allows for accurate real-time sensing and treatment of bacterial biofilms within a single domain, thus facilitating a significant decrease in device footprint and reduction in additional bulky equipment. The IDE sensors were demonstrated to detect biofilm growth in real time. Using the measured impedance change and user inputs, the latter of which is provided through a convenient and simple graphical interface, the MATLAB module intelligently switches the system from sensing into treatment mode. Treatment was performed by temporarily applying a 100 mV signal, for only a small fraction of the total treatment period, across the same IDEs in combination with small doses of antibiotic. This microsystem thus provides two approaches for BE treatment: first by removing biofilms through periodic low energy BE treatment applied concurrently while monitoring the biofilms through impedimetric measurements and second through the temporary application of higher energy BE signals for short periods of time triggered by the threshold activation of the biofilm growth itself. In the future we envision the use of this integrated system for removal of biofilm infections on medical implants such as urinary tract catheters and artificial joints and even on environmental biofilms such as those found in water pipes. Such application of BE, both during and in response to biofilm growth, will ultimately enable effective rapid and autonomous in situ infection management, thus preventing postsurgery infections and significantly improving the quality of life for millions of patients.

ASSOCIATED CONTENT

Supporting Information

The Supporting Information is available free of charge on the ACS Publications website at DOI: 10.1021/acsami.7b04828.

MATLAB graphical user interface (GUI) control module user inputs and modes of operation; MATLAB control module verification; experimental results for PBS conditioning, biofilm growth, and biofilm treatment (PDF)

AUTHOR INFORMATION

Corresponding Authors

*S.S.: e-mail, dr.sowmya.subramanian@gmail.com; phone, +1 (617)-248-4786; address, University of Maryland, 2226 Kim Engineering Building, College Park, MD 20742, U.S.

*R.G.: e-mail, ghodssi@umd.edu; phone, +1 (301) 405-8158; fax, +1 (301) 314-9920; address, University of Maryland, 2173 A. V. Williams Building, College Park, MD 20742, U.S.

ORCID

Sowmya Subramanian: 0000-0001-9953-5790

Author Contributions

The manuscript was written through contributions of all authors. All authors have given approval to the final version of the manuscript.

Funding

The authors thank the Robert W. Deutsch Foundation for financial support. The authors also acknowledge the funding support provided by NSF (CBET Grant 1160005, CBET Grant 1264509) and DTRA (Grant S0924-4247(15)30249-1HDTRA1-13-1-00037).

Notes

The authors declare no competing financial interest.

ACKNOWLEDGMENTS

We thank Dr. Hadar Ben-Yoav for constructive consultations during this work. The authors appreciate the support of the Maryland Nanocenter and its Fablab staff. The authors also acknowledge Kathryn Schneider for useful discussions.

REFERENCES

(1) Harris, L. G.; Richards, R. G. Staphylococci and Implant Surfaces: A Review. *Injury* **2006**, *37* (2, Suppl.), S3−S14.

(2) Donlan, R. M.; Costerton, J. W. Biofilms: Survival Mechanisms of Clinically Relevant Microorganisms. *Clin Microbiol Rev.* **2002**, *15* (2), 167−193.

(3) Costerton, J. W.; Stewart, P. S.; Greenberg, E. P. Bacterial Biofilms: A Common Cause of Persistent Infections. *Science* **1999**, *284* (5418), 1318−1322.

(4) Ghannoum, M.; O'Toole, G. A. *Microbial Biofilms*; ASM Press, 2004.

(5) Surette, M. G.; Miller, M. B.; Bassler, B. L. Quorum Sensing in Escherichia Coli, Salmonella Typhimurium, and Vibrio Harveyi: A New Family of Genes Responsible for Autoinducer Production. *Proc. Natl. Acad. Sci. U. S. A.* **1999**, *96* (4), 1639−1644.

(6) Miller, M. B.; Bassler, B. L. Quorum Sensing in Bacteria. *Annu. Rev. Microbiol.* **2001**, *55* (1), 165−199.

(7) Waters, C. M.; Bassler, B. L. Quorum Sensing: Cell-to-Cell Communication in Bacteria. *Annu. Rev. Cell Dev. Biol.* **2005**, *21*, 319−346.

(8) Anderl, J. N.; Franklin, M. J.; Stewart, P. S. Role of Antibiotic Penetration Limitation in Klebsiella Pneumoniae Biofilm Resistance to Ampicillin and Ciprofloxacin. *Antimicrob. Agents Chemother.* **2000**, *44* (7), 1818−1824.

(9) Anderson, G. G.; O'Toole, G. A. Innate and Induced Resistance Mechanisms of Bacterial Biofilms. In *Bacterial Biofilms*; Springer, 2008; pp 85−105.

(10) Kumon, H.; Tomochika, K. i.; Matunaga, T.; Ogawa, M.; Ohmori, H. A Sandwich Cup Method for the Penetration Assay of Antimicrobial Agents through Pseudomonas Exopolysaccharides. *Microbiol. Immunol.* **1994**, *38* (8), 615−619.

(11) Bose, S.; Ghosh, A. K. Biofilms: A Challenge to Medical Science. *J. Clin. Diagn. Res.* **2013**, *5* (1), 127−130.
(12) Walters, M. C.; Roe, F.; Bugnicourt, A.; Franklin, M. J.; Stewart, P. S. Contributions of Antibiotic Penetration, Oxygen Limitation, and Low Metabolic Activity to Tolerance of Pseudomonas Aeruginosa Biofilms to Ciprofloxacin and Tobramycin. *Antimicrob. Agents Chemother.* **2003**, *47* (1), 317−323.
(13) Fux, C. A.; Stoodley, P.; Hall-Stoodley, L.; Costerton, J. W. Bacterial Biofilms: A Diagnostic and Therapeutic Challenge. *Expert Rev. Anti-Infect. Ther.* **2003**, *1* (4), 667−683.
(14) Fux, C. A.; Stoodley, P.; Shirtliff, M.; Costerton, J. W. The Functional Resistance of Bacterial Biofilms. In *Antimicrobial Drug Resistance*; Springer, 2009; pp 121−131.
(15) del Pozo, J. L.; Patel, R. The Challenge of Treating Biofilm-Associated Bacterial Infections. *Clin. Pharmacol. Ther.* **2007**, *82* (2), 204−209.
(16) Subramanian, S.; Aschenbach, K. H.; Evangelista, J. P.; Najjar, M. B.; Song, W.; Gomez, R. D. Rapid, Sensitive and Label-Free Detection of Shiga-Toxin Producing Escherichia Coli O157 Using Carbon Nanotube Biosensors. *Biosens. Bioelectron.* **2012**, *32* (1), 69−75.
(17) Rodrigues Ribeiro Teles, F. S.; Pires de Távora Tavira, L. A.; Pina da Fonseca, L. J. Biosensors as Rapid Diagnostic Tests for Tropical Diseases. *Crit. Rev. Clin. Lab. Sci.* **2010**, *47* (3), 139−169.
(18) Mir, M.; Homs, A.; Samitier, J. Integrated Electrochemical DNA Biosensors for Lab-on-a-Chip Devices. *Electrophoresis* **2009**, *30* (19), 3386−3397.
(19) Hobson, N. S.; Tothill, I.; Turner, A. P. F. Microbial Detection. *Biosens. Bioelectron.* **1996**, *11* (5), 455−477.
(20) Ivnitski, D.; Abdel-Hamid, I.; Atanasov, P.; Wilkins, E. Biosensors for Detection of Pathogenic Bacteria. *Biosens. Bioelectron.* **1999**, *14* (7), 599−624.
(21) Philip-Chandy, R.; Scully, P. J.; Eldridge, P.; Kadim, H.; Grapin, M. G.; Jonca, M. G.; D'Ambrosio, M. G.; Colin, F. An Optical Fiber Sensor for Biofilm Measurement Using Intensity Modulation and Image Analysis. *IEEE J. Sel. Top. Quantum Electron.* **2000**, *6* (5), 764−772.
(22) Muñoz-Berbel, X.; Muñoz, F. J.; Vigués, N.; Mas, J. On-Chip Impedance Measurements to Monitor Biofilm Formation in the Drinking Water Distribution Network. *Sens. Actuators, B* **2006**, *118* (1−2), 129−134.
(23) Oliver, L. M.; Dunlop, P. S. M.; Byrne, J. A.; Blair, I. S.; Boyle, M.; McGuigan, K. G.; McAdams, E. T. An Impedimetric Sensor for Monitoring the Growth of Staphylococcus Epidermidis. In *Engineering in Medicine and Biology Society, 2006 EMBS '06 28th Annual International Conference of the IEEE*; IEEE, 2006; pp 535−538.
(24) Schofield, A. L.; Rudd, T. R.; Martin, D. S.; Fernig, D. G.; Edwards, C. Real-Time Monitoring of the Development and Stability of Biofilms of Streptococcus Mutans Using the Quartz Crystal Microbalance with Dissipation Monitoring. *Biosens. Bioelectron.* **2007**, *23* (3), 407−413.
(25) Zikmund, A.; Ripka, P.; Krasny, L.; Judl, T.; Jahoda, D. Biofilm Detection by the Impedance Method. In *3rd International Conference on Biomedical Engineering and Informatics (BMEI)*; IEEE, 2010; 1432−1434. DOI: 10.1109/BMEI.2010.5639411.
(26) Bruchmann, J.; Sachsenheimer, K.; Rapp, B. E.; Schwartz, T. Multi-Channel Microfluidic Biosensor Platform Applied for Online Monitoring and Screening of Biofilm Formation and Activity. *PLoS One* **2015**, *10* (2), e0117300.
(27) Becerro, S.; Paredes, J.; Mujika, M.; Lorenzo, E. P.; Arana, S. Electrochemical Real-Time Analysis of Bacterial Biofilm Adhesion and Development by Means of Thin-Film Biosensors. *IEEE Sens. J.* **2016**, *16* (7), 1856−1864.
(28) Yuan, Y.; Guo, T.; Qiu, X.; Tang, J.; Huang, Y.; Zhuang, L.; Zhou, S.; Li, Z.; Guan, B.-O.; Zhang, X.; Albert, J. Electrochemical Surface Plasmon Resonance Fiber-Optic Sensor: In Situ Detection of Electroactive Biofilms. *Anal. Chem.* **2016**, *88* (15), 7609−7616.
(29) Stepanović, S.; Vuković, D.; Dakić, I.; Savić, B.; Švabić-Vlahović, M. A Modified Microtiter-Plate Test for Quantification of Staphylococcal Biofilm Formation. *J. Microbiol. Methods* **2000**, *40* (2), 175−179.
(30) Tamachkiarow, A.; Flemming, H. On-Line Monitoring of Biofilm Formation in a Brewery Water Pipeline System with a Fibre Optical Device. *Water Sci. Technol.* **2003**, *47* (5), 19−24.
(31) Kim, Y. W.; Sardari, S. E.; Meyer, M. T.; Iliadis, A. A.; Wu, H. C.; Bentley, W. E.; Ghodssi, R. An Ald Aluminum Oxide Passivated Surface Acoustic Wave Sensor for Early Biofilm Detection. *Sens. Actuators, B* **2012**, *163* (1), 136−145.
(32) Berkenpas, E.; Millard, P.; Da Cunha, M. P. Detection of Escherichia Coli O157: H7 with Langasite Pure Shear Horizontal Surface Acoustic Wave Sensors. *Biosens. Bioelectron.* **2006**, *21* (12), 2255−2262.
(33) Silley, P.; Forsythe, S. Impedance Microbiology—A Rapid Change for Microbiologists. *J. Appl. Bacteriol.* **1996**, *80* (3), 233−243.
(34) Yang, L.; Bashir, R. Electrical/Electrochemical Impedance for Rapid Detection of Foodborne Pathogenic Bacteria. *Biotechnol. Adv.* **2008**, *26* (2), 135−150.
(35) Yang, L.; Li, Y.; Griffis, C. L.; Johnson, M. G. Interdigitated Microelectrode (Ime) Impedance Sensor for the Detection of Viable Salmonella Typhimurium. *Biosens. Bioelectron.* **2004**, *19* (10), 1139−1147.
(36) Varshney, M.; Li, Y. Double Interdigitated Array Microelectrode-Based Impedance Biosensor for Detection of Viable Escherichia Coli O157:H7 in Growth Medium. *Talanta* **2008**, *74* (4), 518−525.
(37) Gosheger, G.; Hardes, J.; Ahrens, H.; Streitburger, A.; Buerger, H.; Erren, M.; Gunsel, A.; Kemper, F. H.; Winkelmann, W.; von Eiff, C. Silver-Coated Megaendoprostheses in a Rabbit Model—An Analysis of the Infection Rate and Toxicological Side Effects. *Biomaterials* **2004**, *25* (24), 5547−5556.
(38) Hetrick, E. M.; Schoenfisch, M. H. Reducing Implant-Related Infections: Active Release Strategies. *Chem. Soc. Rev.* **2006**, *35* (9), 780−789.
(39) Hardes, J.; Ahrens, H.; Gebert, C.; Streitbuerger, A.; Buerger, H.; Erren, M.; Gunsel, A.; Wedemeyer, C.; Saxler, G.; Winkelmann, W.; Gosheger, G. Lack of Toxicological Side-Effects in Silver-Coated Megaprostheses in Humans. *Biomaterials* **2007**, *28* (18), 2869−2875.
(40) Reddy, S. T.; Chung, K. K.; McDaniel, C. J.; Darouiche, R. O.; Landman, J.; Brennan, A. B. Micropatterned Surfaces for Reducing the Risk of Catheter-Associated Urinary Tract Infection: An in Vitro Study on the Effect of Sharklet Micropatterned Surfaces to Inhibit Bacterial Colonization and Migration of Uropathogenic Escherichia coli. *J. Nephrol Endourol* **2011**, *25* (9), 1547−1552.
(41) Harris, L. G.; Tosatti, S.; Wieland, M.; Textor, M.; Richards, R. G. Staphylococcus Aureus Adhesion to Titanium Oxide Surfaces Coated with Non-Functionalized and Peptide-Functionalized Poly(L-Lysine)-Grafted-Poly(Ethylene Glycol) Copolymers. *Biomaterials* **2004**, *25* (18), 4135−4148.
(42) Del Curto, B.; Brunella, M. F.; Giordano, C.; Pedeferri, M. P.; Valtulina, V.; Visai, L.; Cigada, A. Decreased Bacterial Adhesion to Surface-Treated Titanium. *Int. J. Artif. Organs* **2005**, *28* (7), 718−730.
(43) Li, J. X.; Wang, J.; Shen, L. R.; Xu, Z. J.; Li, P.; Wan, G. J.; Huang, N. The Influence of Polyethylene Terephthalate Surfaces Modified by Silver Ion Implantation on Bacterial Adhesion Behavior. *Surf. Coat. Technol.* **2007**, *201* (19−20), 8155−8159.
(44) Smith, K. M.; Bu, Y.; Suga, H. Induction and Inhibition of Pseudomonas Aeruginosa Quorum Sensing by Synthetic Autoinducer Analogs. *Chem. Biol.* **2003**, *10* (1), 81−89.
(45) Rasmussen, T. B.; Givskov, M. Quorum-Sensing Inhibitors as Anti-Pathogenic Drugs. *Int. J. Med. Microbiol.* **2006**, *296* (2−3), 149−161.
(46) Roy, V.; Smith, J. A.; Wang, J.; Stewart, J. E.; Bentley, W. E.; Sintim, H. O. Synthetic Analogs Tailor Native Ai-2 Signaling across Bacterial Species. *J. Am. Chem. Soc.* **2010**, *132* (32), 11141−11150.
(47) Costerton, J. W.; Ellis, B.; Lam, K.; Johnson, F.; Khoury, A. E. Mechanism of Electrical Enhancement of Efficacy of Antibiotics in Killing Biofilm Bacteria. *Antimicrob. Agents Chemother.* **1994**, *38* (12), 2803−2809.

DOI: 10.1021/acsami.7b04828
ACS Appl. Mater. Interfaces 2017, 9, 31362−31371

(48) Wellman, N.; Fortun, S. M.; McLeod, B. R. Bacterial Biofilms and the Bioelectric Effect. *Antimicrob. Agents Chemother.* **1996**, *40* (9), 2012−2014.
(49) Stoodley, P.; DeBeer, D.; Lappin-Scott, H. M. Influence of Electric Fields and pH on Biofilm Structure as Related to the Bioelectric Effect. *Antimicrob. Agents Chemother.* **1997**, *41* (9), 1876−1879.
(50) Shirtliff, M. E.; Bargmeyer, A.; Camper, A. K. Assessment of the Ability of the Bioelectric Effect to Eliminate Mixed-Species Biofilms. *Appl. Environ. Microbiol.* **2005**, *71* (10), 6379−6382.
(51) Del Pozo, J. L.; Rouse, M. S.; Patel, R. Bioelectric Effect and Bacterial Biofilms. A Systematic Review. *Int. J. Artif. Organs* **2008**, *31* (9), 786−795.
(52) Kim, Y. W.; Meyer, M. T.; Berkovich, A.; Subramanian, S.; Iliadis, A. A.; Bentley, W. E.; Ghodssi, R. A Surface Acoustic Wave Biofilm Sensor Integrated with a Treatment Method Based on the Bioelectric Effect. *Sens. Actuators, A* **2016**, *238*, 140−149.
(53) Kim, Y. W.; Mosteller, M. P.; Subramanian, S.; Meyer, M. T.; Bentley, W. E.; Ghodssi, R. An Optical Microfluidic Platform for Spatiotemporal Biofilm Treatment Monitoring. *J. Micromech. Microeng.* **2016**, *26* (1), 015013.
(54) Del Pozo, J. L.; Rouse, M. S.; Mandrekar, J. N.; Steckelberg, J. M.; Patel, R. The Electricidal Effect: Reduction of Staphylococcus and Pseudomonas Biofilms by Prolonged Exposure to Low-Intensity Electrical Current. *Antimicrob. Agents Chemother.* **2009**, *53* (1), 41−45.
(55) Khoury, A. E.; Lam, K.; Ellis, B.; COSTERTON, J. W. Prevention and Control of Bacterial Infections Associated with Medical Devices. *ASAIO J.* **1992**, *38* (3), 174−178.
(56) Blenkinsopp, S. A.; Khoury, A.; Costerton, J. Electrical Enhancement of Biocide Efficacy against Pseudomonas aeruginosa Biofilms. *Appl. Environ. Microbiol.* **1992**, *58* (11), 3770−3773.
(57) Paredes, J.; Becerro, S.; Arizti, F.; Aguinaga, A.; Del Pozo, J. L.; Arana, S. Real Time Monitoring of the Impedance Characteristics of Staphylococcal Bacterial Biofilm Cultures with a Modified Cdc Reactor System. *Biosens. Bioelectron.* **2012**, *38* (1), 226−232.
(58) Paredes, J.; Becerro, S.; Arizti, F.; Aguinaga, A.; Del Pozo, J. L.; Arana, S. Interdigitated Microelectrode Biosensor for Bacterial Biofilm Growth Monitoring by Impedance Spectroscopy Technique in 96-Well Microtiter Plates. *Sens. Actuators, B* **2013**, *178*, 663−670.
(59) Paredes, J.; Becerro, S.; Arana, S. Label-Free Interdigitated Microelectrode Based Biosensors for Bacterial Biofilm Growth Monitoring Using Petri Dishes. *J. Microbiol. Methods* **2014**, *100*, 77−83.
(60) Subramanian, S.; Gerasopoulos, K.; Guo, M.; Sintim, H. O.; Bentley, W. E.; Ghodssi, R. Autoinducer-2 Analogs and Electric Fields—An Antibiotic-Free Bacterial Biofilm Combination Treatment. *Biomed. Microdevices* **2016**, *18* (5), 1−12.
(61) Roy, V.; Meyer, M. T.; Smith, J. A. I.; Gamby, S.; Sintim, H. O.; Ghodssi, R.; Bentley, W. E. Ai-2 Analogs and Antibiotics: A Synergistic Approach to Reduce Bacterial Biofilms. *Appl. Microbiol. Biotechnol.* **2013**, *97* (6), 2627−2638.
(62) Wang, L.; Li, J.; March, J. C.; Valdes, J. J.; Bentley, W. E. Luxs-Dependent Gene Regulation in Escherichia Coli K-12 Revealed by Genomic Expression Profiling. *J. Bacteriol.* **2005**, *187* (24), 8350−8360.
(63) Meyer, M. T.; Roy, V.; Bentley, W. E.; Ghodssi, R. Development and Validation of a Microfluidic Reactor for Biofilm Monitoring Via Optical Methods. *J. Micromech. Microeng.* **2011**, *21* (5), 054023.
(64) Di Biasio, A.; Cametti, C. On the Dielectric Relaxation of Biological Cell Suspensions: The Effect of the Membrane Electrical Conductivity. *Colloids Surf., B* **2011**, *84* (2), 433−441.
(65) Asami, K. Characterization of Heterogeneous Systems by Dielectric Spectroscopy. *Prog. Polym. Sci.* **2002**, *27* (8), 1617−1659.
(66) Cametti, C. Dielectric and Conductometric Properties of Highly Heterogeneous Colloidal Systems. *Riv. Nuovo Cimento Soc. Ital. Fis.* **2009**, *32* (5), 185−260.
(67) Asami, K.; Hanai, T.; KoIzumi, N. Dielectric Analysis of Escherichia Coli Suspensions in the Light of the Theory of Interfacial Polarization. *Biophys. J.* **1980**, *31* (2), 215−228.
(68) Park, S.; Zhang, Y.; Wang, T.-H.; Yang, S. Continuous Dielectrophoretic Bacterial Separation and Concentration from Physiological Media of High Conductivity. *Lab Chip* **2011**, *11* (17), 2893−2900.
(69) Korth, B.; Rosa, L. F.; Harnisch, F.; Picioreanu, C. A Framework for Modeling Electroactive Microbial Biofilms Performing Direct Electron Transfer. *Bioelectrochemistry* **2015**, *106* (Part A), 194−206.
(70) Wu, J.; Lian, M.; Yang, K. Micropumping of Biofluids by Alternating Current Electrothermal Effects. *Appl. Phys. Lett.* **2007**, *90* (23), 234103.
(71) Van Gerwen, P.; Laureyn, W.; Laureys, W.; Huyberechts, G.; Op De Beeck, M.; Baert, K.; Suls, J.; Sansen, W.; Jacobs, P.; Hermans, L.; Mertens, R. Nanoscaled Interdigitated Electrode Arrays for Biochemical Sensors. *Sens. Actuators, B* **1998**, *49* (1−2), 73−80.
(72) Kim, Y. W.; Subramanian, S.; Gerasopoulos, K.; Ben-Yoav, H.; Wu, H.-C.; Quan, D.; Carter, K.; Meyer, M. T.; Bentley, W. E.; Ghodssi, R. Effect of Electrical Energy on the Efficacy of Biofilm Treatment Using the Bioelectric Effect. *Npj Biofilms Microbiomes* **2015**, *1*, 15016.

DOI: 10.1021/acsami.7b04828
ACS Appl. Mater. Interfaces 2017, 9, 31362−31371